Driven inelastic Maxwell gases

V. V. Prasad,[1] Sanjib Sabhapandit,[1] and Abhishek Dhar[2]

[1]*Raman Research Institute, Bangalore 560080, India*
[2]*International Centre for Theoretical Sciences, TIFR, Bangalore 560012, India*

We consider the inelastic Maxwell model, which consists of a collection of particles that are characterized by only their velocities and evolving through binary collisions and external driving. At any instant, a particle is equally likely to collide with any of the remaining particles. The system evolves in continuous time with mutual collisions and driving taken to be point processes with rates τ_c^{-1} and τ_w^{-1}, respectively. The mutual collisions conserve momentum and are inelastic, with a coefficient of restitution r. The velocity change of a particle with velocity v, due to driving, is taken to be $\Delta v = -(1 + r_w)v + \eta$, where $r_w \in [-1,1]$ and η is Gaussian white noise. For $r_w \in (0,1]$, this driving mechanism mimics the collision with a randomly moving wall, where r_w is the coefficient of restitution. Another special limit of this driving is the so-called Ornstein-Uhlenbeck process given by $\frac{dv}{dt} = -\Gamma v + \eta$. We show that while the equations for the n-particle velocity distribution functions ($n = 1, 2, \dots$) do not close, the joint evolution equations of the variance and the two-particle velocity correlation functions close. With the exact formula for the variance we find that, for $r_w \neq -1$, the system goes to a steady state. Also we obtain the exact tail of the velocity distribution in the steady state. On the other hand, for $r_w = -1$, the system does not have a steady state. Similarly, the system goes to a steady state for the Ornstein-Uhlenbeck driving with $\Gamma \neq 0$, whereas for the purely diffusive driving ($\Gamma = 0$), the system does not have a steady state.

I. INTRODUCTION

A gas of particles undergoing elastic collisions evolves to an equilibrium state where the single-particle velocity distribution is Gaussian (Maxwell distribution). For such an isolated system, the collisions merely distribute energy among the particles while keeping the total energy constant. In contrast, if the collisions between particles are inelastic, the system dissipates energy upon collisions; the change of energy in each binary collision is given by $\Delta E = -\frac{1}{2}(1 - r^2)[\frac{1}{2}m(\Delta v)^2]$, where r is the coefficient of restitution, m is the mass of the particles, and Δv is the relative velocity along the direction of the collision. It is indeed possible to go from an inelastic to a quasielastic system of particles within the same experimental setup using tunable repulsive interactions [1]. In a system of inelastic gas starting from a spatially homogeneous state, the total energy initially decreases according to the famous Haff's law [2] with $E(t) = E_0(1 + t/t_*)^{-2}$, where $t_* \propto (1 - r^2)^{-1}$. At long times the particles form high-density clusters [3] with typical mass growing with time as $M \sim t^\delta$. In this late time regime, the conservation of momentum dictates that the energy of the system decreases with time as $E(t) \sim t^{-\delta}$. In one dimension, in this late time regime, the inelastic gas behaves like a perfectly inelastic sticky gas (ballistic aggregation model), which can be described by the inviscid Burgers equation [4]. For the sticky gas, scaling arguments [5] as well as exact calculation [6] gives $\delta = 2/3$. There is no exact calculation for higher dimensions, and the validity of scaling arguments as well as the Burgers-like equation is not clear [7,8].

In order to keep an inelastic gas in a steady state, it is clearly necessary to inject energy into the system. It has been found that, if energy injection (heating) into the system takes place only at the boundaries, then clustering of the particles still persist in the bulk of the system [9–11], although there is some evidence of nonclustering for rod-shaped objects [12]. These studies indicate the need of uniform heating in order to obtain a spatially homogeneous steady state for regular granular matter. For such a uniformly driven system of inelastic particles, one of the most interesting questions is the velocity distribution in the steady state. Experiments on driven granular systems have found non-Gaussian velocity distributions [13,14]. The velocity distribution found in some of the experiments [15–17] follow the form $P(v) \sim \exp(-A|v|^\alpha)$ with $\alpha \approx 1.5$. Our interest in this paper is in the uniformly driven inelastic granular gas.

In analytical studies based on kinetic theory methods, one constructs the evolution equation for the single-particle velocity distribution function (ignoring spatial correlations for the homogeneous gas). Due to the binary collisions, the equation for the single-particle distribution depends on the two-particle distribution, the two-particle distribution depends on the three-particle distribution, and so on, creating a hierarchy of equations for the probability distributions, similar to the BBGKY hierarchy. Usually one circumvents this problem by invoking the *molecular chaos hypothesis*, which assumes that the colliding particles are uncorrelated before a collision and, hence, factorize the two-particle distribution into two one-particle distributions, resulting in a closed (*Boltzmann*) equation for the single-particle velocity distribution. Modeling the uniform heating by adding a diffusive term in the Boltzmann equation, van Noije and Ernst [18] have calculated the steady-state velocity distribution. They found a stretched exponential tail with $\alpha = 1.5$ for inelastic hard sphere gas (where the collision rate is proportional to the relative velocity of the colliding particles). On the other hand, the numerical studies by van Zon and McKintosh [19] have found a continuous spectrum of possible exponents ranging up to $\alpha < 2$ rather than a universal exponent $\alpha = 1.5$. Intrigued by the differences in the two results, in this paper we investigate one of the simplest, yet nontrivial, models of inelastic gases, namely the Maxwell model.

In the inelastic Maxwell model, introduced by Ben-Naim and Krapivsky [20], the Boltzmann equation for the single-particle velocity distribution (assuming product form of two-point distribution) is further simplified by taking the rate of collision to be independent of the velocities of the colliding particles. In this case it was shown [21,22] that, with the diffusive driving, the steady-state velocity distribution has a form $P(v) \sim \exp(-A|v|)$, while it becomes Gaussian in the elastic limit [23]. Recently [24], we studied a discrete time version of the inelastic Maxwell model and showed that some exact results could be obtained without taking recourse to the molecular chaos hypothesis. In particular, it was observed that the equations for the variance and the two-particle correlations of the velocities close within themselves *exactly*, even though the equations for the velocity distributions have the usual hierarchy. From the exact evolution of these equations, we find that *purely diffusive driving is not enough* to sustain the steady state, as it causes the variance and the correlations to increase linearly with time. This simply follows from the fact that the total momentum of the system also diffuses. As a result, the assumption of "molecular chaos" is invalid. We then showed that this problem has a physically motivated resolution—namely by introducing a different scheme of driving. Wall collisions of vibrated particles do not conserve total momentum and, is the typical way of driving in real systems—we incorporate this into the driving forces and studied the resulting steady state. Importantly, we were also able to obtain the exact tails for the velocity distributions in the steady state.

In this paper, we extend the results of discrete time dynamics to a system evolving in continuous time. For the case of continuous time dynamics, we again illustrate that the evolution equations for the variance and the two-point correlations form a closed set, even though the equations for the distribution functions themselves do not close. An exact mapping to the discrete model enables us to obtain the high-energy tail of the velocity distribution for the continuous time model. We also find that the Ornstein-Uhlenbeck driving is a special case of our model. This makes it possible to obtain the exact tail behavior of the velocity distribution in a steady state when driven by an Ornstein-Uhlenbeck process. Thus our work compliments the previous studies [25–27] where the probability density function (PDF) of the velocity is calculated as a series expansion around the Maxwellian. The exact coupled equations, for the variance and correlation, permits one to predict the existence of steady states in different parameter regimes of the system. In particular, we show the absence of a steady state for a continuous time system driven by purely diffusive driving, which is a special case of the Ornstein-Uhlenbeck process.

The continuous time model, introduced here has another significance in connection with real systems. In experimental studies of driven granular systems, the driving is caused by the collisions of the particles with the vibrating walls of the container. Like interparticle collisions, the wall collisions also occur as a point process in time, with finite change in particle velocities. In contrast, the typical analytical models employ continuous driving schemes like diffusive or Ornstein-Uhlenbeck processes. We propose that the model that is introduced here is a better scheme of driving in the sense that the driving is taken to be a point process in time with a rate associated with it.

The rest of the paper is organized as follows. We first define the rules for the inelastic collision between a pair of particles as well as the driving mechanism in Sec. II. Next, in Sec. III, we discuss the Maxwell gas with continuous time dynamics with both collision and driving occurring as Poisson processes. We find an exact formula for the coupled evolution for the variance and the two-particle correlation function. We also obtain the exact tail of the steady-state velocity distribution in the thermodynamic limit of large number of particles. We point out the correspondence between this continuous time model and the discrete model discussed in Appendix A. In Sec. IV, we take a particular limit of the driving parameters to obtain the Ornstein-Uhlenbeck process. The absence of steady state for a system with diffusive driving is easily obtained from the evolution equations. Finally, we conclude in Sec. V. The Maxwell model evolving with discrete dynamics and some of the details are given in the Appendix.

II. COLLISION RULE AND DRIVING MECHANISM

For simplicity, we assume the velocities of the particles to be single component (one dimensional). In the inelastic collisions between two particles (say, i and j), their velocities are modified from (v_i^*, v_j^*) to (v_i, v_j) according to $(v_i - v_j) = -r(v_i^* - v_j^*)$ while keeping the total momentum unchanged $v_i + v_j = v_i^* + v_j^*$, where r is the coefficient of restitution and we have set the masses of the particles to unity. Combining the above two rules, one gets the postcollision velocities in terms of the precollision velocities as

$$v_i = \frac{(1-r)}{2}v_i^* + \frac{(1+r)}{2}v_j^*, \tag{1a}$$

$$v_j = \frac{(1+r)}{2}v_i^* + \frac{(1-r)}{2}v_j^*. \tag{1b}$$

Our model of driving is inspired by the collision of particles with a vibrating wall, where the postcollision velocity v_i of a particle is related to its precollision velocity v_i^* by $(v_i - V_w) = -r_w(v_i^* - V_w^*)$, with r_w being the coefficient of restitution between the wall and particle collision. However, the velocity of a massive wall remains unchanged during a collision, $V_w^* = V_w$. Therefore, one has $v_i = -r_w v_i^* + (1 + r_w)V_w$. One can further assume that the velocity of the wall in each collision is an uncorrelated random variable. Therefore, in our model of driving, the velocity of a particle is modified according to

$$v_i = -r_w v_i^* + \eta, \tag{2}$$

where η is a Gaussian random variable with zero mean and variance σ^2, drawn independently at each time.

For physical collisions, the coefficients of restitution $\{r, r_w\} \in [0,1]$, where $\{r, r_w\} = 1$ corresponds to the elastic collision, whereas $\{r, r_w\} = 0$ corresponds to the sticky collision. However, it is important to note that, as a mathematical model of a driven dissipative system, Eqs. (1) and (2) are well defined over the entire range $\{r, r_w\} \in [-1,1]$. Therefore, we

investigate this model over this entire range and treat r_w and σ as independent parameters.

III. THE MAXWELL MODEL

The model consists of a set of N identical particles characterized by only their one-component velocities v_i, with $i = 1, 2, \ldots, N$. The initial velocities are taken independently from a Gaussian distribution. There is no spatial structure in the model. The system evolves in continuous time and we consider both the interparticle collisions and the driving to be uncorrelated random processes in time (see Appendix A for the model with discrete time dynamics). We let the particles of each pair collide at a rate $g\tau_c^{-1}$, according the the collision rule given by Eq. (1). On the other hand, each particle is driven at a rate $g\tau_w^{-1}$, according to the driving mechanism given by Eq. (2).

Let us define a set of distribution functions for the system,

$$F_1(u_1, t) \equiv \sum_{i=1}^{N} \langle \delta(u_1 - v_i(t)) \rangle, \tag{3a}$$

$$F_2(u_1, u_2, t) \equiv \sum_{i=1}^{N} \sum_{j \neq i}^{N} \langle \delta(u_1 - v_i(t))\delta(u_2 - v_j(t)) \rangle, \tag{3b}$$

$$F_3(u_1, u_2, u_3, t) \equiv \sum_{i=1}^{N} \sum_{j \neq i}^{N} \sum_{k \neq i, j}^{N} \langle \delta(u_1 - v_i(t))\delta(u_2 - v_j(t))$$
$$\times \delta(u_3 - v_k(t)) \rangle, \tag{3c}$$

and so on. The evolution equations of the above distributions form a hierarchy, and the first two such equations are given by

$$\frac{\partial}{\partial t} F_1(v_1, t) = g\tau_c^{-1} \left[\int dv_2 \overline{T}(v_1, v_2) F_2(v_1, v_2, t) \right]$$
$$+ g\tau_w^{-1} \left[\int dv_1^* F_1(v_1^*, t) \langle \delta(v_1 - [-r_w v_1^* + \eta_1]) \rangle_{\eta_1} - F_1(v_1, t) \right], \tag{4a}$$

$$\frac{\partial}{\partial t} F_2(v_1, v_2, t) = g\tau_c^{-1} \left[\overline{T}(v_1, v_2) F_2(v_1, v_2, t) + \int dv_3 [\overline{T}(v_1, v_3) + \overline{T}(v_2, v_3)] F_3(v_1, v_2, v_3, t) \right]$$
$$+ g\tau_w^{-1} \left[\int dv_1^* F_2(v_1^*, v_2, t) \langle \delta(v_1 - [-r_w v_1^* + \eta_1]) \rangle_{\eta_1} \right.$$
$$\left. + \int dv_2^* F_2(v_1, v_2^*, t) \langle \delta(v_2 - [-r_w v_2^* + \eta_2]) \rangle_{\eta_2} - 2 F_2(v_1, v_2, t) \right]. \tag{4b}$$

The first square bracket in the right-hand side of Eqs. (4a) and (4b) gives the contribution from the interparticle collisions, with $\overline{T}(v_i, v_j)$ defined as $\overline{T}(v_i, v_j)S(v_i, v_j) = r^{-1}S(v_i^*, v_j^*) - S(v_i, v_j)$. The operator $\overline{T}$ acts only on the two variables designated by the arguments of the operator. The second set of square brackets in Eqs. (4a) and (4b) are the contribution from the driving, where the angular brackets refer to the averaging over the noise distribution. Various approximation schemes have been used in the past to break the hierarchy of similar equations [27,28]. In the following, we show that exact closed set of coupled equations can be obtained for the variance and the two-particle correlation function, whose solution, in turn, can be used to close the hierarchy for the single-particle distribution function in the $N \to \infty$ limit.

The variance and the two-particle correlation function can be obtained using the above-defined distributions as

$$\Sigma_1(t) = \frac{1}{N} \int dv_1 v_1^2 F_1(v_1, t), \tag{5a}$$

$$\Sigma_2(t) = \frac{1}{N(N-1)} \int dv_1 dv_2 v_1 v_2 F_2(v_1, v_2, t). \tag{5b}$$

Now, multiplying Eq. (4a) by v_1^2 and then integrating over v_1 and multiplying Eq. (4b) by $v_1 v_2$ and integrating over both v_1 and v_2 yields a closed set of equations for

$X(t) = [\Sigma_1(t), \Sigma_2(t)]^T$, given by

$$\frac{dX(t)}{dt} = g[\mathbf{R}X(t) + C], \tag{6}$$

where

$$\mathbf{R} = \begin{bmatrix} -\left\{ \frac{(1-r^2)(N-1)}{2\tau_c} + \frac{1-r_w^2}{\tau_w} \right\} & \frac{(1-r^2)(N-1)}{2\tau_c} \\ \frac{(1-r^2)}{2\tau_c} & -\left\{ \frac{(1-r^2)}{2\tau_c} + \frac{2(1+r_w)}{\tau_w} \right\} \end{bmatrix} \tag{7}$$

and $C = [\tau_w^{-1}\sigma^2, 0]^T$. Note that Eq. (6) is exact and no approximation is made in arriving at it from Eq. (4).

Now, in the Maxwell model with the collision rates proportional to the typical velocity [29], one uses $g = \Sigma_1^{1/2}$. However, it makes Eq. (6) nonlinear, and hence, the analysis becomes difficult. On the other hand, it is clear from both Eq. (4) and Eq. (6) that the steady-state properties are independent of the choice of g. Therefore, we set $g = 1$ as in Ref. [20], which makes Eq. (6) linear. This would, of course, change the time-dependent properties. For example, in the absence of the driving ($\sigma = 0$), the two cases, $g = \Sigma_1^{1/2}$ and $g = 1$, yield different cooling laws, as discussed in Appendix B and shown in Fig. 1.

In the presence of the driving ($\sigma \neq 0$), one again expects the approach to the steady state to differ for the two choices of g. We analyze Eq. (6) for the particular choice of $g = 1$. In this case, the linear equation can be exactly solved. The variance and the two-particle correlation are given
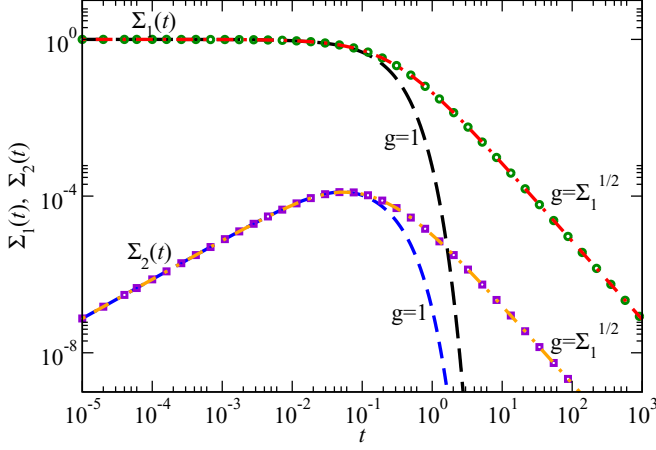
FIG. 1. (Color online) The variance $\Sigma_1(t)$ and the two-particle correlation $\Sigma_2(t)$ of the velocities for a cooling inelastic gas with 1000 particles with $r = 1/2$ in the absence of the driving (static walls) for the two cases: (a) The rate of collision is independent of the variance $g = 1$ and (b) the rate of collision is proportional to the variance $g = \Sigma_1^{1/2}(t)$. For $g = 1$, the lines plot the exact analytical expressions given by Eq. (B1). For $g = \Sigma_1^{1/2}(t)$, the lines plot the approximate expressions given by Eqs. (B5) and (B6), while the points are obtained by exact numerical evaluation of the equation Eq. (B3).

by

$$\Sigma_1(t) = \frac{\Sigma_1(0)}{\lambda_+ - \lambda_-}[(R_{22} - \lambda_-)e^{-\lambda_- t} + (\lambda_+ - R_{22})e^{-\lambda_+ t}]$$
$$+ \frac{\tau_w^{-1}\sigma^2}{\lambda_+ - \lambda_-}\left[\frac{R_{22} - \lambda_-}{\lambda_-}(1 - e^{-\lambda_- t})\right.$$
$$\left. + \frac{\lambda_+ - R_{22}}{\lambda_+}(1 - e^{-\lambda_+ t})\right], \quad \text{and} \quad (8a)$$

$$\Sigma_2(t) = \frac{\Sigma_1(0)R_{21}}{\lambda_+ - \lambda_-}[e^{-\lambda_- t} - e^{-\lambda_+ t}]$$
$$+ \frac{\tau_w^{-1}\sigma^2 R_{21}}{\lambda_+ - \lambda_-}\left[\frac{1}{\lambda_-}(1 - e^{-\lambda_- t}) - \frac{1}{\lambda_+}(1 - e^{-\lambda_+ t})\right], \quad (8b)$$

respectively, where $-\lambda_\pm$ are the eigenvalues of $\mathbf{R}$, given by Eq. (B2), and $R_{ij} = |\mathbf{R}_{ij}|$.

Now, for the case $r_w = -1$, one of the eigenvalues of $\mathbf{R}$ becomes zero ($\lambda_- = 0$), while the other is negative ($\lambda_+ = R_{11} + R_{22} > 0$). For these particular values of $\lambda_\pm$, the above expressions become

$$\Sigma_1(t) = \frac{\Sigma_1(0)}{\lambda_+}[R_{22} + R_{11}e^{-\lambda_+ t}] + \frac{\sigma^2}{\tau_w}\frac{R_{11}}{\lambda_+^2}[1 - e^{-\lambda_+ t}]$$
$$+ \frac{\sigma^2}{\tau_w}\frac{R_{22}}{\lambda_+}t, \quad (9a)$$

$$\Sigma_2(t) = \frac{\Sigma_1(0)R_{21}}{\lambda_+}[1 - e^{-\lambda_+ t}] - \frac{\sigma^2}{\tau_w}\frac{R_{21}}{\lambda_+^2}[1 - e^{-\lambda_+ t}]$$
$$+ \frac{\sigma^2}{\tau_w}\frac{R_{21}}{\lambda_+}t. \quad (9b)$$

Thus, both $\Sigma_1(t)$, and $\Sigma_2(t)$ eventually increase linearly with time and the system does not have a steady state for $r_w = -1$ when the driving is present ($\sigma \neq 0$), which is shown in Fig. 2.

On the other hand, for $-1 < r_w \leqslant 1$, since both the eigenvalues of $\mathbf{R}$ are negative ($\lambda_\pm > 0$) (see Appendix B), the system reaches a steady state as shown in Fig. 3. The steady state values of Σ_1 and Σ_2 can be obtained by either taking the limit of $t \to \infty$ in Eq. (8) or by setting the left-hand side of Eq. (6) to zero. From the latter, it is clear that the steady-state values are independent of the choice of g. We denote the steady-state values of the variance and the two-particle correlation by Σ_1^{ss} and Σ_2^{ss}, respectively, and they are given by

$$\Sigma_1^{ss} = \frac{\sigma^2[(1 - r^2) + 4(1 + r_w)(\tau_c/\tau_w)]}{(1 - r_w^2)(1 - r^2) + 2(1 + r_w)[(1 - r^2)(N - 1) + 2(1 - r_w^2)(\tau_c/\tau_w)]}, \quad (10a)$$

$$\Sigma_2^{ss} = \frac{\sigma^2(1 - r^2)}{(1 - r_w^2)(1 - r^2) + 2(1 + r_w)[(1 - r^2)(N - 1) + 2(1 - r_w^2)(\tau_c/\tau_w)]}. \quad (10b)$$

We now analyze the above expressions for various relative rates τ_c/τ_w. Let us take $\tau_c/\tau_w \sim N^\xi$ for large N, where ξ is a real number. From Eq. (10), we observe that for $\xi < 0$, both Σ_1^{ss} and Σ_2^{ss} vanish as $O(1/N)$ for large N. Similarly, for $0 < \xi < 1$, they again vanish as $\Sigma_1^{ss} \sim O(1/N^{1-\xi})$ and $\Sigma_2^{ss} \sim O(1/N)$ for large N. Only for $\xi \geqslant 1$ do we get a nonzero steady-state variance for large N, given by

$$\Sigma_1^{ss} = \frac{2\sigma^2(\tau_c/\tau_w)}{N(1 - r^2) + 2(1 - r_w^2)(\tau_c/\tau_w)}, \quad (11)$$

whereas the two-particle correlation function vanishes as $\Sigma_2^{ss} \sim O(1/N^\xi)$.

Due to the mean-field nature of the problem, it is reasonable to assume that the rate, τ_c^{-1}, of interparticle collisions is

inversely proportional to the total number of pairs [$\tau_c \propto N(N - 1)/2$] whereas the rate, τ_w^{-1}, of driving is inversely proportional to the total number of particles ($\tau_w \propto N$). This is analogous to taking the coupling constant proportional to $1/N$ in infinite-ranged spin models. Indeed, if we set $\tau_c/\tau_w = \gamma(N - 1)$, then Eq. (10) becomes identical to those obtained for the discrete time dynamics [see Eq. (A4)]. In particular, in the limit $N \to \infty$, the steady-state variance becomes independent of N,

$$\Sigma_1^{ss} = \frac{2\gamma\sigma^2}{(1 - r^2) + 2\gamma(1 - r_w^2)}. \quad (12)$$

Moreover, since the two-particle correlation function vanishes in the limit of large N, we can factorize the multiparticle
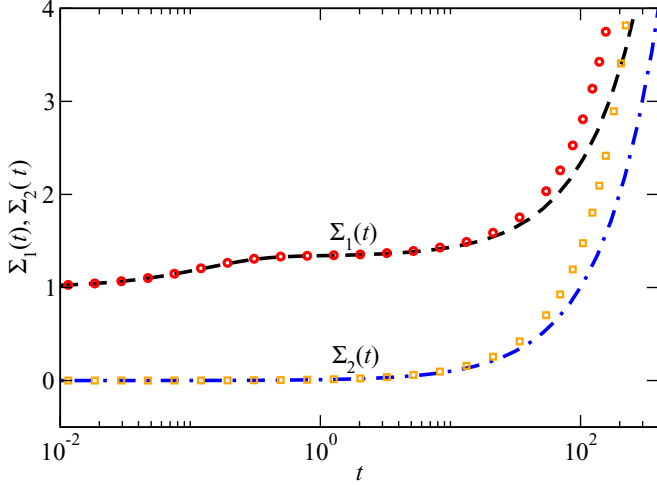
FIG. 2. (Color online) The variance $\Sigma_1(t)$ and the two-particle correlation $\Sigma_2(t)$ of the velocities, for an inelastic gas with 1000 particles with $r = 1/2$ driven by wall collisions with $\sigma = 1$ and $r_w = -1$ for the two cases: (a) The rate of collision is independent of the variance $g = 1$ and (b) the rate of collision is proportional to the variance $g = \Sigma_1^{1/2}(t)$. For $g = 1$, the lines plot the exact analytical expressions given by Eq. (9). For $g = \Sigma_1^{1/2}(t)$, the points are obtained by exact numerical evaluation of the equation Eq. (6).

distribution functions in terms of the single-particle distribution function in Eq. (4), e.g., $F_2(v_1, v_2) = F_1(v_1) F_1(v_2)$. Therefore, in the steady state [the time derivatives in Eq. (4) are zero], multiplying Eq. (4a) by $\exp(-\lambda v_1)$ and then integrating over v_1 we obtain the equation satisfied by the generating function $Z(\lambda)$ as

$$Z(\lambda) = q Z(\epsilon \lambda) Z([1 - \epsilon]\lambda) + (1 - q) Z(r_w \lambda) f(\lambda), \quad (13)$$
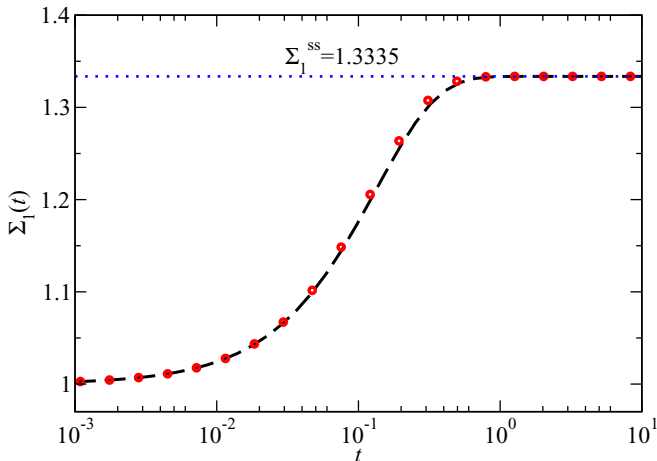

FIG. 3. (Color online) The variance $\Sigma_1(t)$ of the velocities for an inelastic gas with 1000 particles with $r = 1/2$ driven by wall collisions with $\sigma = 1$ and $r_w = 1$ for the two cases: (a) The rate of collision is independent of the variance $g = 1$ and (b) the rate of collision is proportional to the variance $g = \Sigma_1^{1/2}(t)$. For $g = 1$, the line plots the exact analytical expressions given by Eq. (8). For $g = \Sigma_1^{1/2}(t)$, the points are obtained by exact numerical evaluation of the equation Eq. (6). The dotted line highlights the steady-state value calculated from Eq. 10(a).

where $q = 1/(1 + \gamma)$ and $f(\lambda) = \exp(\lambda^2 \sigma^2 / 2)$. Since the velocity distribution is even, we have $Z(-\lambda) = Z(\lambda)$. The above equation is identical to Eq. (A6) obtained for the discrete time dynamics. Therefore, as expected, both the continuous time and the discrete time dynamics yield the same steady state.

For the particular case $r_w = 1$, we can obtain $Z(\lambda)$ as an infinite product involving simple poles by iteratively solving

$$Z(\lambda) = [1 - (1 - q) f(\lambda)]^{-1} q Z(\epsilon \lambda) Z([1 - \epsilon]\lambda).$$

Therefore, the tail of the velocity distribution is exponential $P(v) \sim \exp(-|v|/v^*)$, where v^* is determined by the pole closest to the origin, coming from the prefactor $[1 - (1 - q) f(\lambda)]^{-1}$.

On the other hand, for $|r_w| < 1$, if we assume the form $P(v) \sim \exp(-A \mid v \mid^\alpha)$ for the PDF, then for $\alpha > 1$ the function $Z(\lambda)$ is analytic. If $Z(\lambda)$ is known, then the large deviation tail of the velocity distribution can be obtained by the saddle-point approximation,

$$P(v) \approx \frac{\exp[\mu(\lambda^*) + \lambda^* v]}{\sqrt{2\pi |\mu''(\lambda^*)|}}, \quad (14)$$

where $\mu(\lambda) = \ln Z(\lambda)$ and the saddle point $\lambda^*(v)$ is implicitly given by the equation $\mu'(\lambda^*) = -v$. Now, if near the saddle point $\mu(\lambda) \sim b|\lambda|^\beta$, one finds

$$\lambda^* = -\text{sgn}(v)\left[\frac{|v|}{(b\beta)}\right]^{1/(\beta-1)}. \quad (15)$$

As a result, $P(v) \sim \exp(-A|v|^\alpha)$, where $\alpha = \beta/(\beta - 1)$ and $A = b(\beta - 1)(b\beta)^{-\alpha}$. Therefore, we substitute the ansatz $Z(\lambda) \sim \exp(b|\lambda|^\beta)$ with $\beta > 1$ in Eq. (13). Since $\varepsilon^\beta + (1 - \varepsilon)^\beta < 1$ for $\varepsilon \in (0,1)$ and $\beta > 1$, the first term on the right-hand side of Eq. (13) becomes negligible compared to the left-hand side for large $|\lambda| \sim |v|^{1/(\beta-1)}$. Thus, comparing the exponent of the left-hand side to that of the second term on the right-hand side, we get $\beta = 2$ and $b = (\sigma^2/2)(1 - r_w^2)^{-1}$. This implies the Gaussian tail

$$P(v) \approx \sqrt{\frac{1 - r_w^2}{2\pi \sigma^2}} \exp\left[-\frac{v^2}{2\sigma^2}(1 - r_w^2)\right]. \quad (16)$$

We have verified this result in Ref. [24] for the case of discrete time dynamics. Figure 4 summarizes the results for different case of r_w.
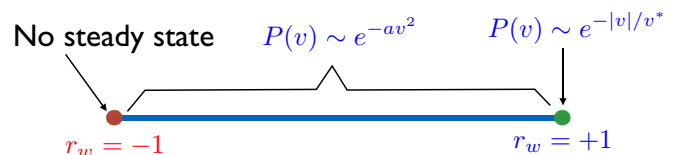

FIG. 4. (Color online) The summary of the results for the PDF of the velocity distribution for different cases of $r_w \in [-1, 1]$. For $r_w = -1$, the system does not reach a steady state, and the average energy and the two-particle correlation eventually increases linearly with the time. For $r_w = 1$, the steady-state PDF has an exponential tail, whereas for $-1 < r_w < 1$, the tail of the PDF for very large velocities is Gaussian.

IV. ORNSTEIN-UHLENBECK DRIVING

We now show that the driving mechanism introduced above becomes an Ornstein-Uhlenbeck process in a special limit. Let us, for the time being, ignore the interparticle collisions and also set $g = 1$. Then Eq. (4a) becomes

$$\frac{\partial F_1(v_1,t)}{\partial t} = \tau_w^{-1}\left[\int dv_1^* F_1(v_1^*,t)\langle\delta(v_1 - [-r_w v_1^* + \eta_1])\rangle_{\eta_1} - F_1(v_1,t)\right]. \quad (17)$$

In terms of the characteristic function, $\widetilde{F}_1(k_1,t) \equiv \int dv_1 F_1(v_1,t) e^{-ik_1 v_1}$, the above equation can be written as

$$\frac{\partial \widetilde{F}_1(k_1,t)}{\partial t} = \tau_w^{-1}\left[\widetilde{F}_1(-k_1 r_w,t) e^{-k^2\sigma^2/2} - \widetilde{F}_1(k_1,t)\right]. \quad (18)$$

The term $\exp(-k^2\sigma^2/2)$ is the characteristic function for a Gaussian noise with variance σ^2. We now consider the limiting case when $\tau_w \to 0$, $\varepsilon_w = (1 + r_w) \to 0$, and $\sigma^2 \to 0$, while keeping appropriate ratios fixed. Replacing r_w with $-(1 - \varepsilon_w)$ in Eq. (18), and expanding and keeping only up to the lowest-order terms in the small parameters, we obtain

$$\frac{\partial \widetilde{F}_1(k_1,t)}{\partial t} = \tau_w^{-1}\left[-\varepsilon_w k_1 \frac{\partial \widetilde{F}_1(k_1,t)}{\partial k_1} - \frac{\sigma^2 k_1^2}{2}\widetilde{F}_1(k_1,t)\right]. \quad (19)$$

Therefore, in the limit $\tau_w \to 0$, $\varepsilon_w \to 0$, and $\sigma^2 \to 0$, while keeping

$$\Gamma = \lim_{\substack{\tau_w \to 0 \\ \varepsilon_w \to 0}} \frac{\varepsilon_w}{\tau_w} \quad \text{and} \quad D = \lim_{\substack{\tau_w \to 0 \\ \sigma^2 \to 0}} \frac{\sigma^2}{2\tau_w} \quad (20)$$

fixed, Eq. (19) becomes

$$\frac{\partial \widetilde{F}_1(k_1,t)}{\partial t} = -\Gamma k_1 \frac{\partial \widetilde{F}_1(k_1,t)}{\partial k_1} - D k_1^2 \widetilde{F}_1(k_1,t). \quad (21)$$

This is nothing but the Fokker-Planck equation of an Ornstein-Uhlenbeck process in the Fourier space, which, in the velocity space, is given by

$$\frac{\partial F_1(v_1,t)}{\partial t} = \Gamma \frac{\partial}{\partial v_1}[v_1 F_1] + D \frac{\partial^2 F_1}{\partial v_1^2}. \quad (22)$$

Thus, in the limit given by Eq. (20), our model of wall driving becomes an Ornstein-Uhlenbeck process, with the parameters defined as in Eq. (20). The matrix $\mathbf{R}$ in this case becomes

$$\mathbf{R} = \begin{bmatrix} -\left\{\frac{(1-r^2)(N-1)}{2\tau_c} + 2\Gamma\right\} & \frac{(1-r^2)(N-1)}{2\tau_c} \\ \frac{(1-r^2)}{2\tau_c} & -\left\{\frac{(1-r^2)}{2\tau_c} + 2\Gamma\right\} \end{bmatrix}, \quad (23)$$

and $C = [2D,0]^T$. The eigenvalues of $\mathbf{R}$ are given by -2Γ and $-2\Gamma - N(1-r^2)/(2\tau_c)$, with the corresponding eigenvectors $[1,1]^T$ and $[1,-1/(N-1)]^T$, respectively. For $g = 1$, we can solve Eq. (6) easily by diagonalizing $\mathbf{R}$. This results in two decoupled equations for the elements of $[y_1(t),y_2(t)]^T =$ $\mathbf{S}^{-1}X$, where

$$\mathbf{S} = \begin{bmatrix} 1 & 1 \\ 1 & -\frac{1}{(N-1)} \end{bmatrix} \quad \text{and} \quad \mathbf{S}^{-1} = \frac{N-1}{N}\begin{bmatrix} \frac{1}{N-1} & 1 \\ 1 & -1 \end{bmatrix}, \quad (24)$$

and $\mathbf{S}^{-1}\mathbf{RS}$ is a diagonal matrix with the eigenvalues of $\mathbf{R}$ being the diagonal elements. It is straightforward to find the solutions as

$$y_1(t) = y_1(0)\exp(-2\Gamma t) + \frac{D}{N\Gamma}[1 - \exp(-2\Gamma t)] \quad (25a)$$

and

$$y_2(t) = y_2(0)\exp\left\{-\left[\frac{N(1-r^2)}{2\tau_c} + 2\Gamma\right]t\right\} + \frac{(N-1)4D\tau_c}{N[N(1-r^2) + 4\Gamma\tau_c]} \times \left(1 - \exp\left\{-\left[\frac{N(1-r^2)}{2\tau_c} + 2\Gamma\right]t\right\}\right). \quad (25b)$$

The initial values, $y_1(0)$ and $y_2(0)$, are obtained in terms of $\Sigma_1(0)$ and $\Sigma_2(0) = 0$. Finally, $\Sigma_1(t)$ and $\Sigma_2(t)$ can be obtained by using $X = \mathbf{S}[y_1(t),y_2(t)]^T$.

Thus, for any nonzero values of Γ, we see from Eq. (25) that as $t \to \infty$, both $y_1(t)$ and $y_2(t)$, and hence $\Sigma_1(t)$ and $\Sigma_2(t)$ approach steady-state values. They are given by

$$\lim_{t \to \infty} \Sigma_1(t) = \frac{D}{\Gamma}\left[\frac{1 - r^2 + 4\Gamma\tau_c}{N(1-r^2) + 4\Gamma\tau_c}\right], \quad (26a)$$

$$\lim_{t \to \infty} \Sigma_2(t) = \frac{D}{\Gamma}\left[\frac{1 - r^2}{N(1-r^2) + 4\Gamma\tau_c}\right]. \quad (26b)$$

These can be also obtained from Eq. (10) by taking the limits given by Eq. (20).

Let us consider the special case, where the dissipative term $\Gamma = 0$. Here the driving is modeled by a Weiner process (diffusive driving), $dv_i/dt = \sqrt{2D}\,\eta_i$. In this case, one of the eigenvalues of $\mathbf{R}$ becomes zero, while the other is $-N(1 - r^2)/(2\tau_c)$. The zero eigenvalue indicates a nonstationary state. The exact solution in the diagonal basis is given by

$$y_1(t) = y_1(0) + \frac{2Dt}{N}, \quad (27a)$$

$$y_2(t) = y_2(0)\exp\left[-\frac{N(1-r^2)t}{2\tau_c}\right] + \frac{(N-1)4D\tau_c}{N^2(1-r^2)}\left[1 - \exp\left(-\frac{N(1-r^2)t}{2\tau_c}\right)\right]. \quad (27b)$$

We can obtain $\Sigma_1(t)$ and $\Sigma_2(t)$ exactly for any time t by inverting $y_1(t)$ and $y_2(t)$. There asymptotic forms for large t are given by

$$\Sigma_1(t) = \frac{\Sigma_1(0)}{N} + \frac{(N-1)4D\tau_c}{N^2(1-r^2)} + \frac{2D}{N}t, \quad (28a)$$

$$\Sigma_2(t) = \frac{\Sigma_1(0)}{N} - \frac{4D\tau_c}{N^2(1-r^2)} + \frac{2D}{N}t. \quad (28b)$$

Since the variance $\Sigma_1(t)$, as well as the two-particle correlation function $\Sigma_2(t)$, eventually grows linearly in time, irrespective of the time scale of collisions and the strength of the driving force, the system does not have a steady state for the diffusive driving. Moreover, the molecular chaos hypothesis becomes invalid as the particles in the system becomes more and more correlated with time.

V. CONCLUSION

In this paper, we have considered a system of Maxwell gas of identical particles evolving under inelastic binary collisions and external driving. We illustrated that even though the hierarchy for the evolution of the distribution functions does not close, those involving the variance and the two-particle correlation of the velocities close exactly—without any approximations. We also find the exact tail of the velocity distribution in the steady state. Both the driving and the interparticle collisions are treated in continuous time as Poisson processes. The Ornstein-Uhlenbeck driving (and so also the diffusive driving) can be realized as a special case. From the exact evolution of the variance and the two-particle correlation function, the conditions for a system to be in a steady state can be obtained. Our calculations show that with the diffusive driving the system cannot have a steady state as the energy and correlations eventually increase linearly with time, as found earlier for discrete time dynamics [24].

APPENDIX A: MAXWELL MODEL WITH DISCRETE TIME DYNAMICS

In this Appendix we briefly review the discrete-time version of the model [24]. The system evolves in discrete time steps as follows. At each time step, with a probability p, a pair of particles (say, i and j) is chosen [of $N(N-1)/2$ pairs] at random and the velocities are modified from (v_i^*, v_j^*) to (v_i, v_j) according to the rule of inelastic collision given by Eq. (1). With the remaining probability $1 - p$, a single particle is selected (of N particles) at random and its velocity is modified according to Eq. (2).

Note that this particular driving scheme differs slightly from the one employed in Ref. [24] where the forcing was done simultaneously on two particles independently. However, this does not alter the qualitative behaviors. Also, unlike the Maxwell model with the rate of collisions proportional to the root-mean-square velocity at that time [29], here the probability p is assumed to be constant over time, as in Ref. [20]. This would, of course, change time-dependent behaviors. For example, as discussed in Appendix B and shown in Fig. 1, in the absence of the external drive, the mean energy decays exponentially, as opposed to the Haff's cooling law. However, our main focus here is in the steady-state properties, which are unchanged even if the collision rates or probabilities are taken to be constant over time; this makes the analysis relatively simpler.

Let $v_i(n)$ be the velocity of the i-th particle at the n-th time step. The variance $\Sigma_1(n)$ and the two-particle correlation function $\Sigma_2(n)$ are defined as

$$\Sigma_1(n) = \frac{1}{N} \sum_{i=1}^{N} \langle v_i^2(n) \rangle, \tag{A1a}$$

$$\Sigma_2(n) = \frac{1}{N(N-1)} \sum_{i \neq j} \langle v_i(n) v_j(n) \rangle, \tag{A1b}$$

respectively, with the angular brackets denoting the ensemble average. It turns out that their evolution follows an exact recursion relation given by

$$X_n = \mathbf{R}_d X_{n-1} + C_d, \tag{A2}$$

where

$$X_n = \begin{bmatrix} \Sigma_1(n) \\ \Sigma_2(n) \end{bmatrix}, \quad C_d = \begin{bmatrix} (1-p)\frac{\sigma^2}{N} \\ 0 \end{bmatrix},$$

and

$$\mathbf{R}_d = \begin{bmatrix} 1 - \frac{\left[p(1-r^2) + (1-p)\left(1-r_w^2\right) \right]}{N} & \frac{p(1-r^2)}{N} \\ \frac{p(1-r^2)}{N(N-1)} & 1 - \frac{\left[p(1-r^2) + 2(N-1)(1-p)(1+r_w) \right]}{N(N-1)} \end{bmatrix}. \tag{A3}$$

Now, for the case $r_w = -1$, one of the eigenvalues of $\mathbf{R}_d$ is unity, resulting in the variance and the two-particle correlation to eventually increase linearly with number of time steps n. Therefore, the system does not reach a steady state for this particular case $r_w = -1$.

Since $\mathbf{R}_d$ is a positive matrix, the Perron-Frobenius theorem guarantees that it has a real positive eigenvalue (Perron-Frobenius eigenvalue) such that the other eigenvalue is strictly less than this, in absolute value. This can be indeed verified easily for a 2×2 matrix by an explicit calculation. The other eigenvalue is also real, which also follows from the fact that the complex eigenvalues of a real matrix must occur in conjugate pairs. The Perron-Frobenius eigenvalue is bounded from above (below) by the maximum (minimum) of the row sums of the matrix. For $-1 < r_w \leqslant 1$, it is immediately evident, from the explicit form of the above matrix, that both the row sums are less than unity. Thus, both the eigenvalues are less than unity, in absolute value, and hence the system reaches a steady state. In the steady state, the variance and the two-particle correlation function can be found as

$$\Sigma_1^{\mathrm{ss}} = \frac{\sigma^2\big[(1-r^2) + 4\gamma(1+r_w)(N-1)\big]}{(1-r_w^2)(1-r^2) + 2(1+r_w)(N-1)\big[(1-r^2) + 2\gamma\big(1-r_w^2\big)\big]}, \tag{A4a}$$

$$\Sigma_2^{\mathrm{ss}} = \frac{\sigma^2(1-r^2)}{(1-r_w^2)(1-r^2) + 2(1+r_w)(N-1)\big[(1-r^2) + 2\gamma\big(1-r_w^2\big)\big]}, \tag{A4b}$$

where $\gamma = (1-p)/(2p)$. In the $N \to \infty$ limit, the steady-state variance, Σ_1^{ss} becomes independent of N,

$$\Sigma_1^{\mathrm{ss}} = \frac{2\gamma\sigma^2}{(1-r^2) + 2\gamma\big(1-r_w^2\big)}, \tag{A5}$$

while the two-particle correlation function Σ_2^{ss} vanishes as $O(N^{-1})$. Therefore, in the limit of large N, the steady-state single-particle probability distribution closes; the moment-generating function $Z(\lambda) = \langle \exp(-\lambda v) \rangle$ of the steady-state velocities can be shown to satisfy the equation

$$Z(\lambda) = q Z(\varepsilon\lambda) Z([1-\varepsilon]\lambda) + (1-q)Z(r_w\lambda)f(\lambda), \quad (A6)$$

where $q = 2p/(1+p)$, $\varepsilon = (1-r)/2$. This equation is identical to Eq. (13) obtained for the continuous time dynamics.

APPENDIX B: HOMOGENEOUS COOLING STATE

Here, we obtain the freely cooling behavior of the system in the absence of driving by setting $C = 0$, (i.e., $\sigma = 0$) in Eq. (6), which mimics a system in a static box. We first consider the linear case $g = 1$ and afterwards consider the case where $g = \Sigma_1^{1/2}$.

1. The linear case: $g = 1$

For $g = 1$, the linear equation (6) with $C = 0$ can be solved exactly, which gives

$$\Sigma_1(t) = \frac{\Sigma_1(0)}{\lambda_+ - \lambda_-}[(R_{22} - \lambda_-)e^{-\lambda_- t} + (\lambda_+ - R_{22})e^{-\lambda_+ t}], \tag{B1a}$$

$$\Sigma_2(t) = \frac{R_{21}\Sigma_1(0)}{\lambda_+ - \lambda_-}[e^{-\lambda_- t} - e^{-\lambda_+ t}], \tag{B1b}$$

where $R_{ij} = |\mathbf{R}_{ij}|$ denote the absolute values of the elements of the matrix $\mathbf{R}$ given by Eq. (7) and $-\lambda_\pm$ are the eigenvalues of the matrix $\mathbf{R}$, given by

$$\lambda_\pm = \tfrac{1}{2}[(R_{11} + R_{22}) \pm \sqrt{(R_{11} + R_{22})^2 - 4(R_{11}R_{22} - R_{12}R_{21})}$$
$$= \tfrac{1}{2}[(R_{11} + R_{22}) \pm \sqrt{(R_{11} - R_{22})^2 + 4R_{12}R_{21}}]. \tag{B2}$$

Note that $\lambda_\pm > 0$ for $-1 < r_w \leqslant 1$. In Fig. 1, we plot $\Sigma_{1,2}$ as a function of t, as given by Eq. (B1).

2. The nonlinear case: $g = \Sigma_1^{1/2}$

In this case, Σ_1 and Σ_2 evolve by

$$\frac{d\Sigma_1}{dt} = -R_{11}\Sigma_1^{3/2} + R_{12}\Sigma_1^{1/2}\Sigma_2, \tag{B3a}$$

$$\frac{d\Sigma_2}{dt} = R_{21}\Sigma_1^{3/2} - R_{22}\Sigma_1^{1/2}\Sigma_2. \tag{B3b}$$

Equation (B3b) for Σ_2 can be solved exactly in terms of Σ_1 as

$$\Sigma_2(t) = R_{21}\int_0^t dt_1 \Sigma_1^{3/2}(t_1) \exp\left[-R_{22}\int_{t_1}^t \Sigma_1^{1/2}(t_2)\,dt_2\right], \tag{B4}$$

where we have used the initial condition $\Sigma_2(0) = 0$. On the other hand, it is difficult to obtain an exact solution of Eq. (B3a) for Σ_1. Nevertheless, near $t = 0$, using the initial condition $\Sigma_2(0) = 0$, we can write Eq. (B3a) as $d\Sigma_1/dt \approx -R_{11}\Sigma_1^{3/2}$, which yields

$$\Sigma_1(t) \approx \frac{\Sigma_1(0)}{\big(1 + \tfrac{1}{2}R_{11}\Sigma_1^{1/2}(0)\,t\big)^2}. \tag{B5}$$

Now, substituting the above expression for $\Sigma_1(t)$ in Eq. (B4), after carrying out the integration, we obtain

$$\Sigma_2(t) \approx \frac{R_{21}/R_{11}}{1-\theta}\left\{P\frac{\Sigma_1(0)}{\big[1 + \tfrac{1}{2}R_{11}\Sigma_1^{1/2}(0)\,t\big]^{2\theta}} - \Sigma_1(t)\right\}, \tag{B6}$$

for $\theta \neq 1$, where $\theta = R_{22}/R_{11}$. For $\theta = 1$, we get

$$\Sigma_2(t) \approx \frac{2(R_{21}/R_{11})\,\Sigma_1(0)\,\ln\big[1 + \tfrac{1}{2}R_{11}\Sigma_1^{1/2}(0)\,t\big]}{\big[1 + \tfrac{1}{2}R_{11}\Sigma_1^{1/2}(0)\,t\big]^2}. \tag{B7}$$

Therefore, for large t, we have $\Sigma_2(t) \sim t^{-2\theta}$ for $\theta < 1$, whereas $\Sigma_2(t) \sim t^{-2}$ for $\theta > 1$. For $\theta = 1$, there is a logarithmic correction $\Sigma_2(t) \sim (\ln t)t^{-2}$.

Now, if we take τ_c to be proportional to the total number of pairs and τ_w to be proportional to the number particles, then for large N, we have τ_c is $O(N^{-2})$ and τ_w is $O(N^{-1})$. Consequently, we see from Eq. (7) that R_{11}, R_{12}, and R_{22} are $O(N^{-1})$, whereas R_{21} is $O(N^{-2})$. Therefore, the prefactor outside the square bracket in the expression (B6)

is $O(N^{-1})$, and hence the second term on the right-hand side of Eq. (B3a) can be neglected even beyond the small t region, for large N. As a result, the expression (B5) and hence Eq. (B6) remain valid even for large times. Essentially, for the freely cooling gas, the two-particle correlation is not important. In the limit $N \to \infty$, the exponent θ is given by

$$\theta = \frac{4\gamma(1 + r_w)}{1 - r^2 + 2\gamma\left(1 - r_w^2\right)}. \tag{B8}$$

Figure 1 compares the expressions (B5) and (B6) with the exact values obtained by numerically solving Eq. (B3).

---

[1] S. Merminod, M. Berhanu, and E. Falcon, Europhys. Lett **106**, 44005 (2014).

[2] P. K. Haff, J. Fluid Mech. **134**, 401 (1983).

[3] I. Goldhirsch and G. Zanetti, Phys. Rev. Lett. **70**, 1619 (1993).

[4] E. Ben-Naim, S. Y. Chen, G. D. Doolen, and S. Redner, Phys. Rev. Lett. **83**, 4069 (1999).

[5] G. F. Carnevale, Y. Pomeau, and W. R. Young, Phys. Rev. Lett. **64**, 2913 (1990).

[6] L. Frachebourg, Phys. Rev. Lett. **82**, 1502 (1999).

[7] X. Nie, E. Ben-Naim, and S. Chen, Phys. Rev. Lett. **89**, 204301 (2002).

[8] S. N. Pathak, Z. Jabeen, D. Das, and R. Rajesh, Phys. Rev. Lett **112**, 038001 (2014).

[9] Y. Du, H. Li, and L. P. Kadanoff, Phys. Rev. Lett. **74**, 1268 (1995).

[10] S. E. Esipov and T. Pöschel, J. Stat. Phys. **86**, 1385 (1997).

[11] E. Opsomer, F. Ludewig, and N. Vandewalle, Europhys. Lett. **99**, 40001 (2012).

[12] K. Harth, U. Kornek, T. Trittel, U. Strachauer, S. Höme, K. Will, and R. Stannarius, Phys. Rev. Lett. **110**, 144102 (2013).

[13] J. S. Olafsen and J. S. Urbach, Phys. Rev. E **60**, R2468(R) (1999).

[14] A. Kudrolli and J. Henry, Phys. Rev. E **62**, R1489(R) (2000).

[15] W. Losert, D. G. W. Cooper, J. Delour, A. Kudrolli, and J. P. Gollub, Chaos **9**, 682 (1999).

[16] F. Rouyer and N. Menon, Phys. Rev. Lett. **85**, 3676 (2000).

[17] I. S. Aranson and J. S. Olafsen, Phys. Rev. E **66**, 061302 (2002).

[18] T. P. C. van Noije and M. H. Ernst, Granul. Matter **1**, 57 (1998).

[19] J. S. van Zon and F. C. MacKintosh, Phys. Rev. Lett. **93**, 038001 (2004); Phys. Rev. E **72**, 051301 (2005).

[20] E. Ben-Naim and P. L. Krapivsky, Phys. Rev. E **61**, R5 (2000).

[21] T. Antal, M. Droz, and A. Lipowski, Phys. Rev. E **66**, 062301 (2002).

[22] A. Santos and M. H. Ernst, Phys. Rev. E **68**, 011305 (2003).

[23] A. Barrat, E. Trizac, and M. H. Ernst, J. Phys. A: Math. Theor. **40**, 4057 (2007).

[24] V. V. Prasad, S. Sabhapandit, and A. Dhar, Europhys. Lett. **104**, 54003 (2013).

[25] A. Puglisi, V. Loreto, U. M. B. Marconi, A. Petri, and A. Vulpiani, Phys. Rev. Lett. **81**, 3848 (1998); A. Puglisi, V. Loreto, U. Marini Bettolo Marconi, and A. Vulpiani, Phys. Rev. E **59**, 5582 (1999).

[26] Umberto Marini Bettolo Marconi and A. Puglisi, Phys. Rev. E **66**, 011301 (2002).

[27] G. Costantini, U. Marini Bettolo Marconi, and A. Puglisi, J. Stat. Mech.: Theory Exp. (2007) P08031.

[28] J. J. Brey, M. I. García de Soria, P. Maynar, and M. J. Ruiz-Montero, Phys. Rev. E **70**, 011302 (2004).

[29] E. Ben-Naim and P. L. Krapivsky, Phys. Rev. E **66**, 011309 (2002).